IMPROVING CO_2 PHOTO-CONVERSION BY LAYERED MATERIALS: BOOSTED OPTO-ELECTRONIC PERFORMANCE AND CATALYTIC ACTIVITY OF g-C_3N_4 BY ULTRASOUND EXFOLIATION

Matteo Tommasi[a], Ehsan Abbasi[a], Mohammad I. Alam[a], Daniele Marinotto[b], Ilenia Rossetti[a,b,*], Gianguido Ramis[c]

[a] Chemical Plants and Industrial Chemistry Group, Dip. Chimica, Università degli Studi di Milano, via C. Golgi 19, 20133 Milan, Italy

[b] INSTM Unit Milano-Università, via C. Golgi 19, 20133 Milan, Italy

[c] Institute of Chemical Sciences and Technologies "Giulio Natta" (SCITEC) of CNR, via Golgi 19, 20133, Milano, Italy

[d] Dip. Ing. Chimica, Civile ed Ambientale, Università degli Studi di Genova, via all'Opera Pia 15A, 16145 Genoa, Italy

[e] INSTM Unit Genova, via all'Opera Pia 15A, 16145 Genoa, Italy

SUPPLEMENTARY INFORMATION

* Corresponding author: ilenia.rossetti@unimi.it

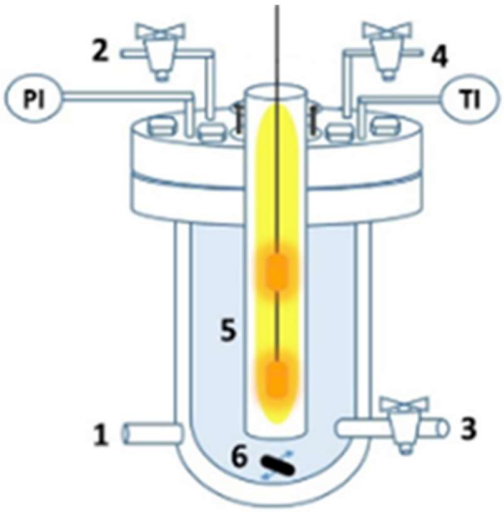

Figure S0. Sketch of high-pressure photo-reactor, adapted and reproduced from [1] under the Creative commons licence.

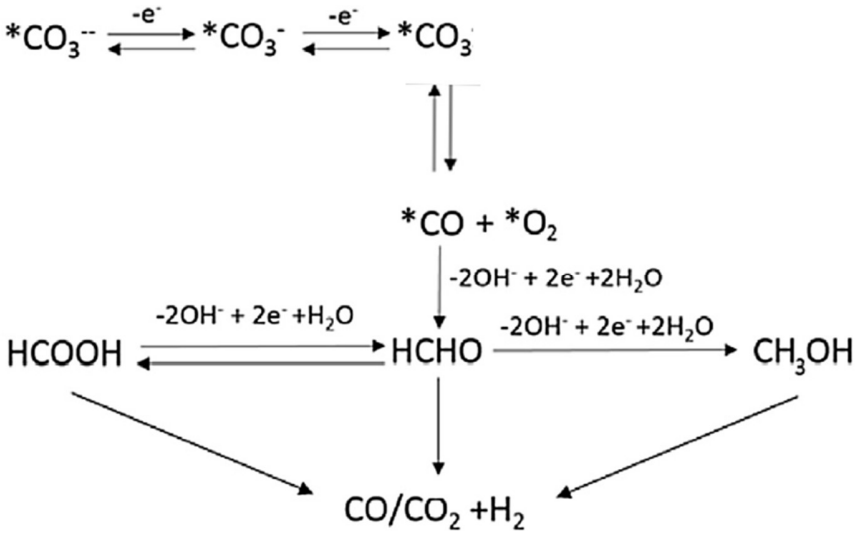

Scheme S1. Scheme of products formation during photoreduction of CO_2 at pH = 14. Reproduced from [6] under the Creative Commons Attribution (CC BY) license.

Transmission Electron Microscopy

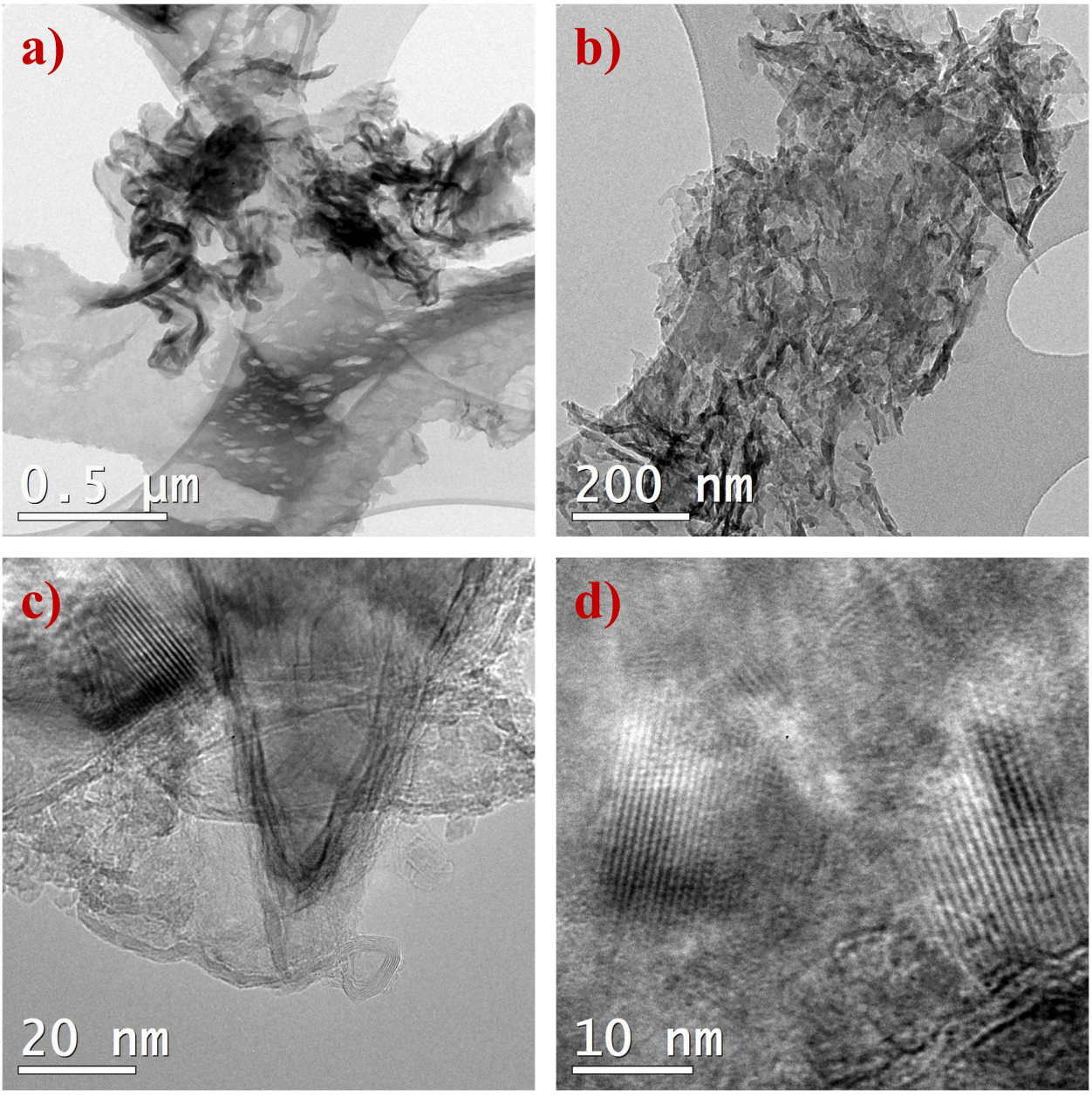

Figure S1. TEM images of GC550 bulk at different magnifications.

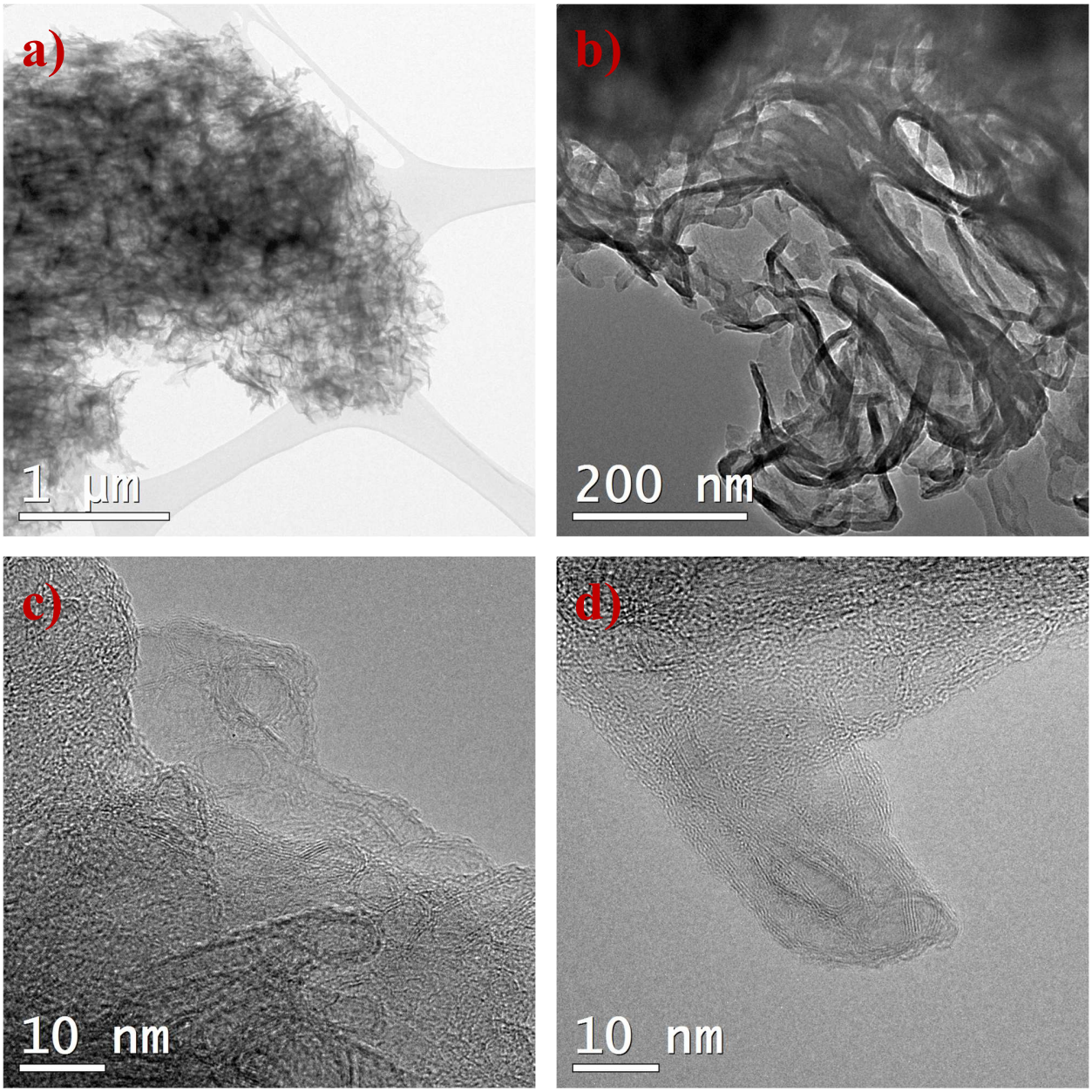

Figure S2. TEM images of exfoliated GC550-120W at different magnifications.

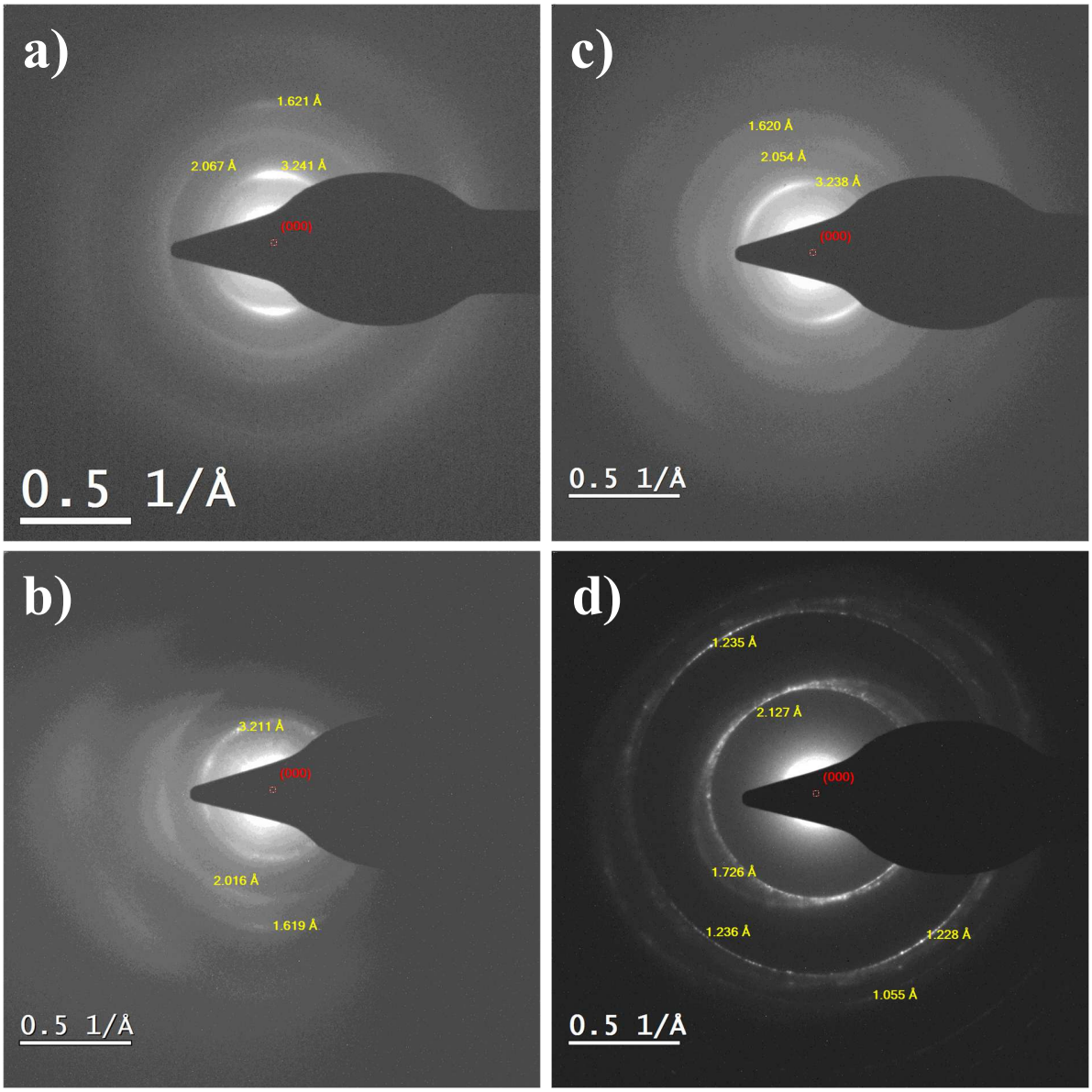

Figure S3. Diffraction patterns of a) and b) GC550; c) and d) GC550-120W

Photophysical properties

Evaluation of the band gap energy by Tauc plot method.

In the case of a sample in powders, the diffuse reflectance spectroscopy (DRS) is the most appropriate experimental technique which allows to determine the value of the band gap energy (E_g) by Tauc plot method. Using DRS, the Tauc plot can be obtained from calculating the Kubelka-Munk or remission function, $F(R_\infty)$, according to the following equations:

$$R_\infty = \frac{R_{sample}}{R_{standard}}$$

$$F(R_\infty) = \frac{K}{S} = \frac{(1 - R_\infty)^2}{2R_\infty}$$

$$F(R_\infty)\, h\nu = C\left(h\nu - E_g\right)^n$$

where R_∞ is the reflectance of the sample for "infinite thickness" (sample thicknesses >1 mm) equal to the ratio of the reflectance of the sample (R_{sample}) and reflectance of the standard material ($R_{standard}$), K and S are the absorption and scattering Kubelka-Munk coefficients, respectively, C is an energy independent constant, h is the Planck constant, ν is the frequency of the incident photon and n is a coefficient that depends on the kind of involved electronic transition, being: n = 1/2 for direct allowed transition, n = 3/2 for direct forbidden transition, n = 2 for indirect allowed transition, and n = 3 for indirect forbidden transition.

For those samples that do not displace an onset in Tauc plot ($[F(R_\infty)\, h\nu]^{1/n}$ vs hν), the E_g is obtained from the extrapolation of the linear least squares fit of $[F(R_\infty)\, h\nu]^{1/n}$ to zero; otherwise, a double-linear fitting must be used in the extrapolation of $[F(R_\infty)\, h\nu]^{1/n}$ to avoid underestimation of the E_g value.[1]

Note: Before recording the diffuse reflectance spectra, the powders of our samples were mixed with the reflectance reference ($BaSO_4$) in a mortar at about 50 % weight ratios. This is a common practice widely used in the optical characterization of strongly absorbing materials, based on the fact that reflectance is only sensitive to the relative amount of the absorbing material. The dilution with $BaSO_4$ does not modify the shape of the spectrum, with differences accounting only for the higher reflectance value as the amount of non-absorbing matrix is raised; moreover, the Kubelka–Munk function is still applicable since the

sample/$BaSO_4$ mixture is pressed in millimetric sample holder at "infinite thickness" and does not transmit any light. Consequentially, in the Tauc plot the shape of $[F(R_\infty)\ h\nu]^{1/n}$ does not change with the dilution ratio, there is only a vertical translation of the function; therefore, applying a double-linear fitting in the extrapolation of $[F(R_\infty)\ h\nu]^{1/n}$ the E_g value can be estimated and more important this value does not depend on the dilution ratio [2].

As observed in the previous note, since the E_g value evaluated by Tauc plot method depends only on the shape of $[F(R_\infty)\ h\nu]^{1/n}$ and since the sample/$BaSO_4$ mixtures were approximately 50 % weight ratios, we have decided to normalize the Kubelka–Munk function ($F_N(R_\infty)$) to get a better comparison of results and subsequently to apply the Tauc plot with a double-linear fitting in the extrapolation of $[F_N(R_\infty)\ h\nu]^{1/n}$ to estimate the E_g value.

Photoluminescence properties

Time-resolved fluorescence curves were fitted using a multi-exponential function:

$$I(\lambda, t) = \sum_{i=1}^{n} \alpha_i(\lambda) \exp\left(\frac{-t}{\tau_i}\right)$$

where *n* is the number of exponentials, $\alpha_i\ (\lambda)$ is the amplitude at wavelength λ and τ_i is the lifetime of the component *i*. The quality of the fit was evaluated through the reduced χ^2 values. In case of multi-exponential decay, it is possible define an average lifetime as [3]:

$$\tau_{av} = \frac{\sum_{i=1}^{n} \alpha_i \tau_i^2}{\sum_{i=1}^{n} \alpha_i \tau_i}$$

A description of the experimental setup and measurement method of the absolute photoluminescence quantum yield (Φ) can be found in the article of K. Suzuki et al. [4] Φ is calculated through Equation:

$$\Phi = \frac{PN\ (Em)}{PN\ (Abs)} = \frac{\int \frac{\lambda}{hc}\left[I_{em}^{sample}(\lambda) - I_{em}^{reference}(\lambda)\right] d\lambda}{\int \frac{\lambda}{hc}\left[I_{exc}^{sample}(\lambda) - I_{exc}^{reference}(\lambda)\right] d\lambda}$$

where PN(Em) is the number of emitted photons, PN(Abs) the number of absorbed photons, λ the wavelength, h the Planck constant, c the speed of light, I_{em}^{sample} and $I_{em}^{reference}$ are the photoluminescence intensities of the sample and reference, respectively, I_{exc}^{sample} and $I_{exc}^{reference}$ are the excitation light

intensities of the sample and reference, respectively. PN(Em) is calculated in the wavelength interval [λ_i, λ_f], where λ_i is taken 10 nm above the excitation wavelength, while λ_f is the upper end wavelength in the emission spectrum. The error made was estimated at around 5%.

Optical properties of the g-C_3N_4 samples.

Band gap energy (E_g) has been evaluated by Tauc plot ($[F_N(R_\infty)\ h\nu]^{1/n}$ vs $h\nu$) method with coefficient n=2 (indirect transition) for all samples [5]. $F_N(R_\infty)$ is the normalized the Kubelka–Munk function.

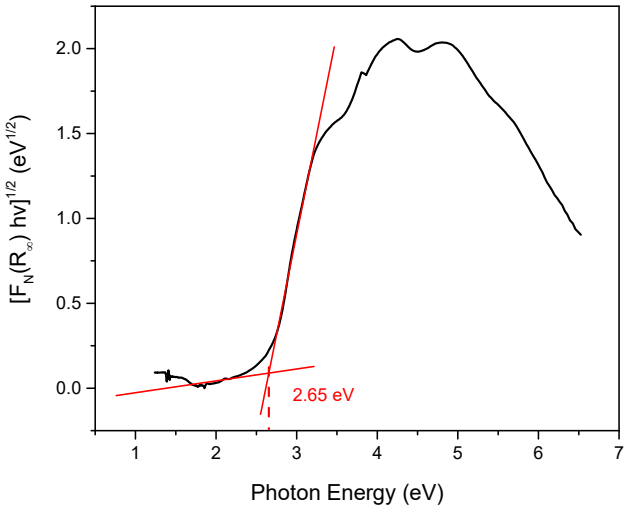

Figure S4. Tauc plot of as-synthesized GC550. Red lines represent the extrapolation of the double linear fitting.

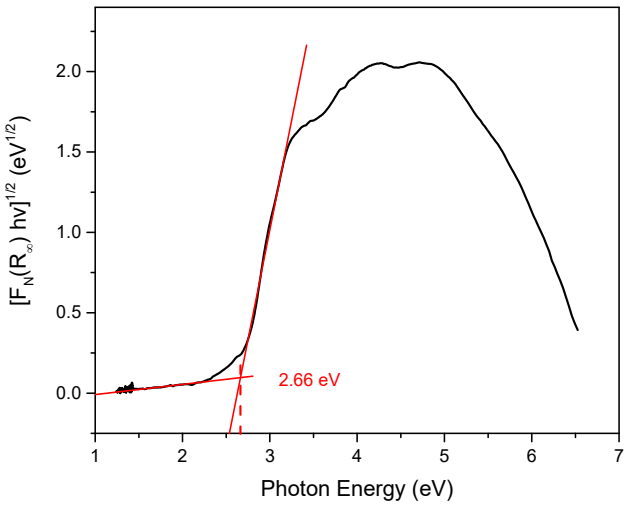

Figure S5. Tauc plot of as-synthesized GC600. Red lines represent the extrapolation of the double linear fitting.

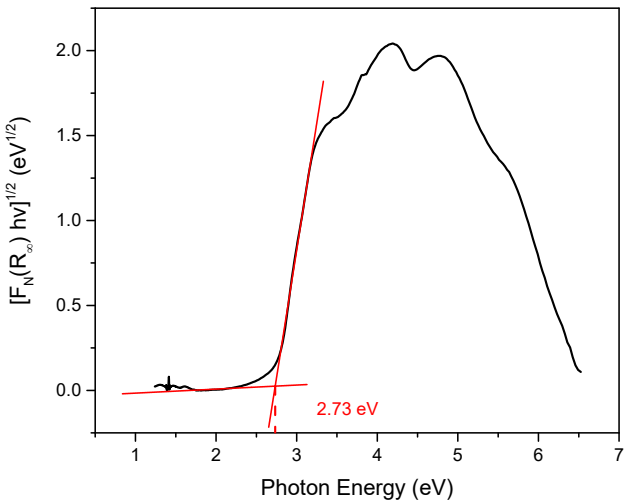

Figure S6. Tauc plot of GC550-30W. Red lines represent the extrapolation of the double linear fitting.

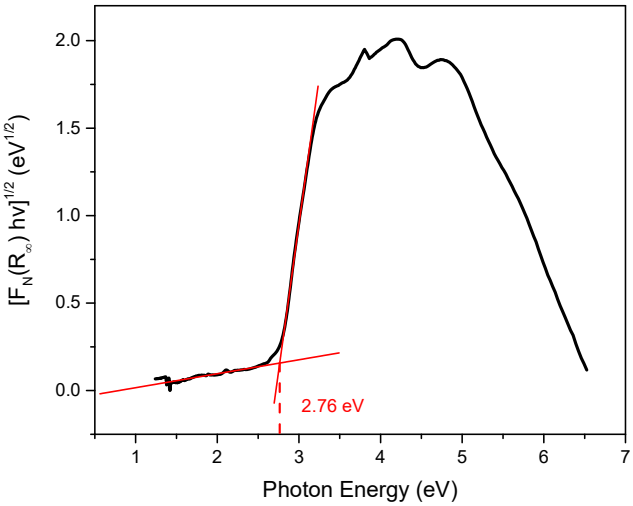

Figure S7. Tauc plot of GC550-60W. Red lines represent the extrapolation of the double linear fitting.

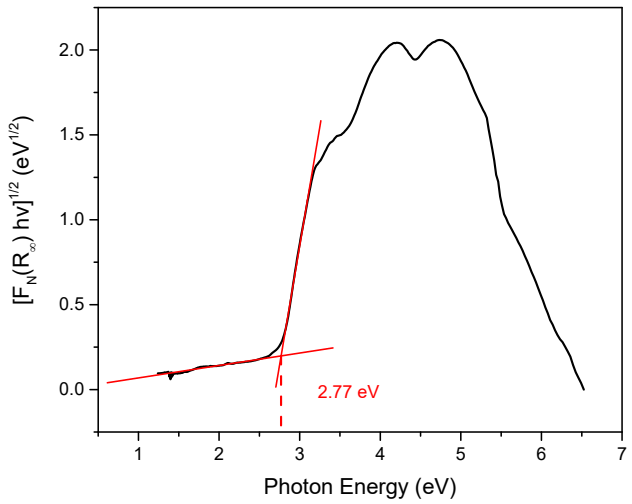

Figure S8. Tauc plot of GC550-90W. Red lines represent the extrapolation of the double linear fitting.

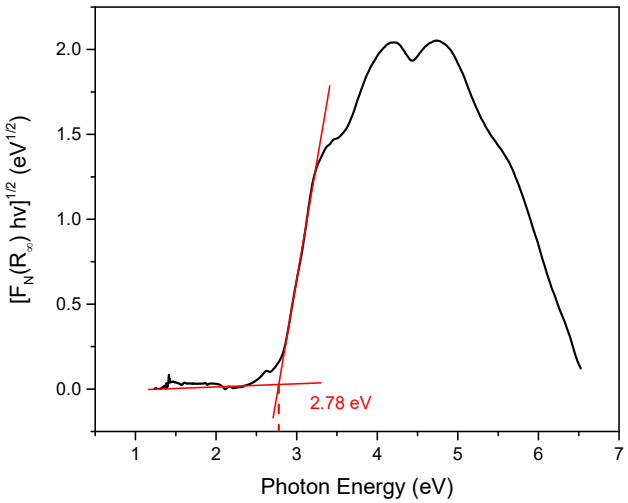

Figure S9. Tauc plot of GC550-120W. Red lines represent the extrapolation of the double linear fitting.

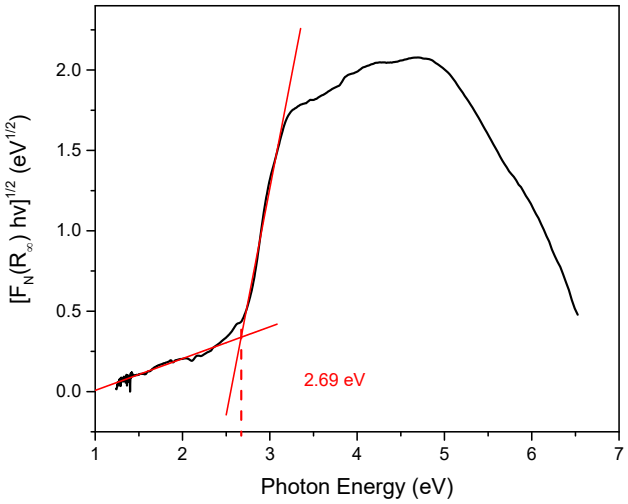

Figure S10. Tauc plot of GC600-120W. Red lines represent the extrapolation of the double linear fitting.

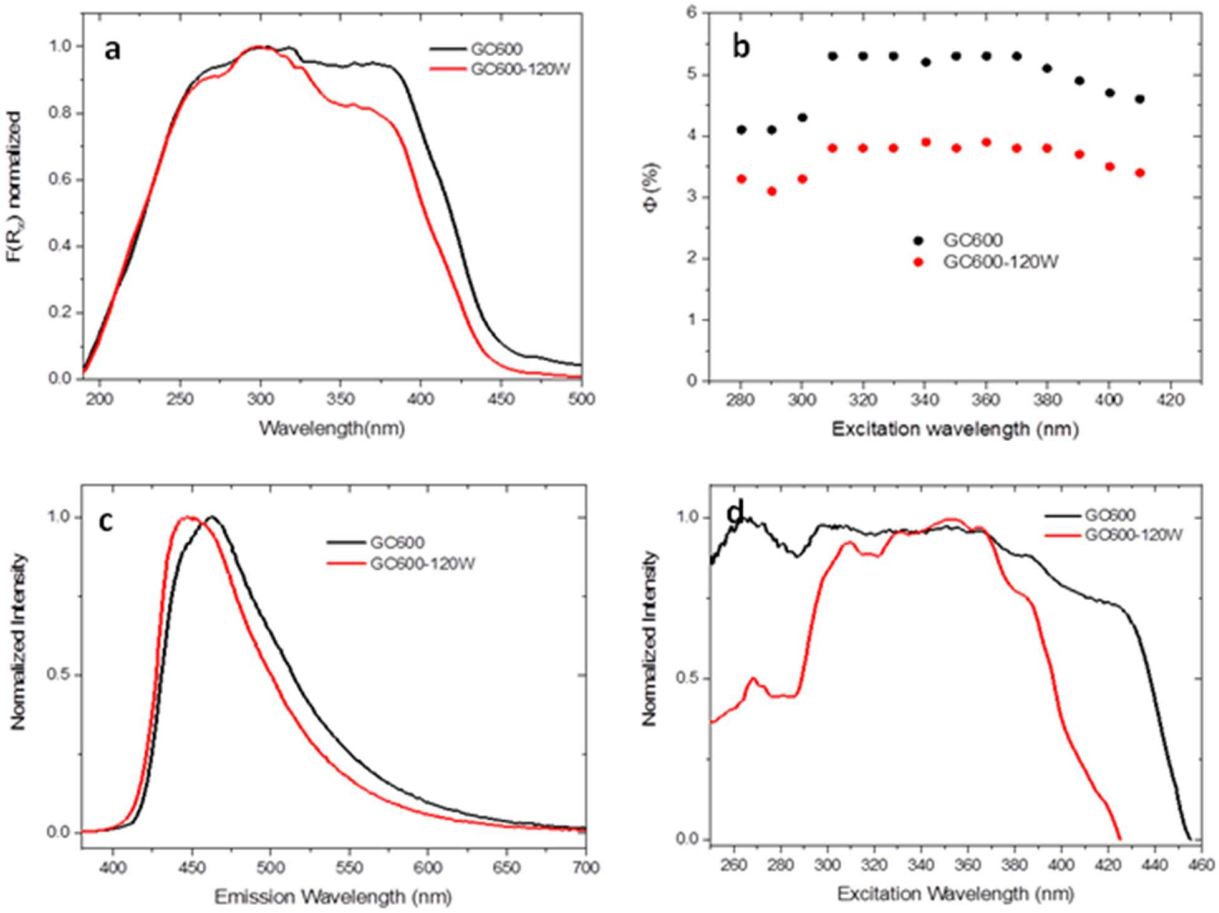

Figure S11. Results obtained from g-C_3N_4 calcined at 600°C: (a) Normalized Kubelka-Munk function (b) Photoluminescence quantum yield (Φ) (c) Normalized emission spectra (Excitation wavelength at 360 nm) and (d) Normalized excitation spectra of the as-synthesized g-C_3N_4 and exfoliated samples.

Time-resolved fluorescence decay measurements obtained exciting at 374 nm at the emission peak of the as-synthesized g-C_3N_4 and exfoliated samples

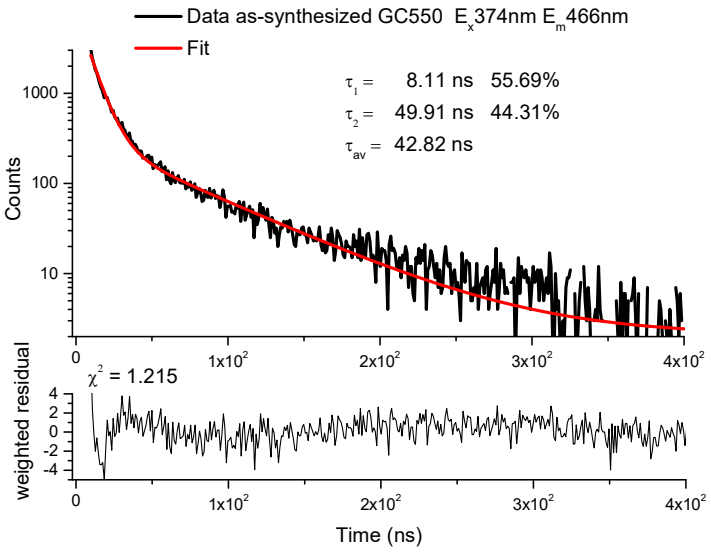

Figure S12. Lifetime measurement of as-synthesized GC550. Emission 466 nm, Excitation 374 nm.

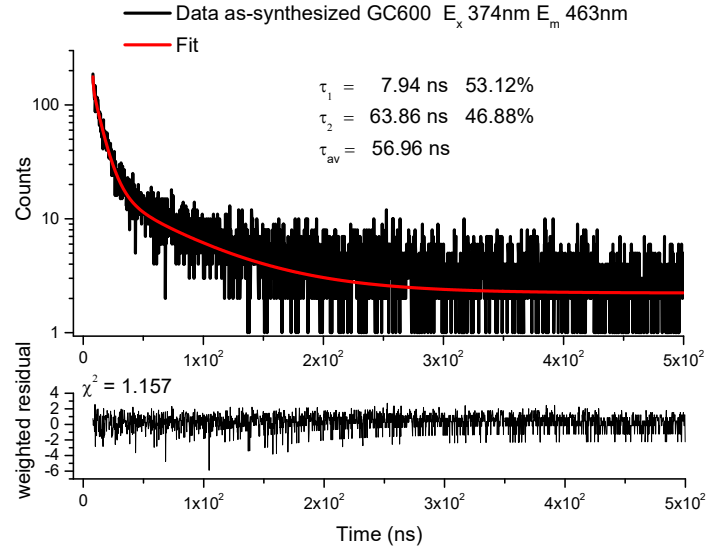

Figure S13. Lifetime measurement of as-synthesized GC600. Emission 463 nm, Excitation 374 nm.

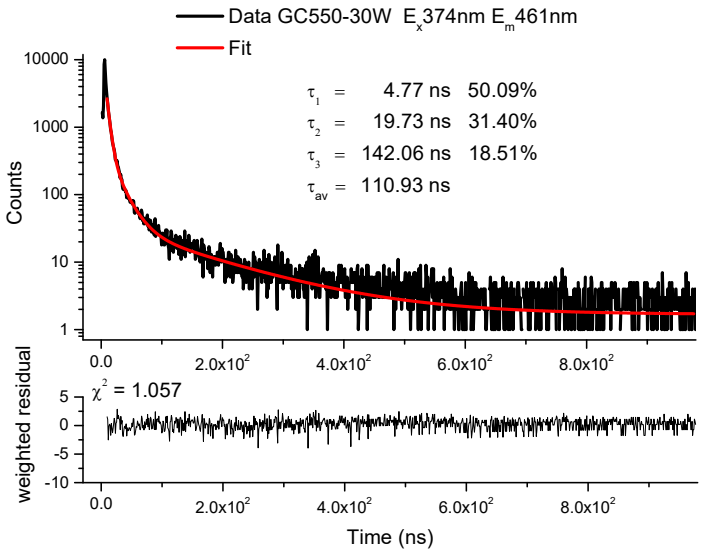

Figure S14. Lifetime measurement of GC550-30W. Emission 461 nm, Excitation 374 nm.

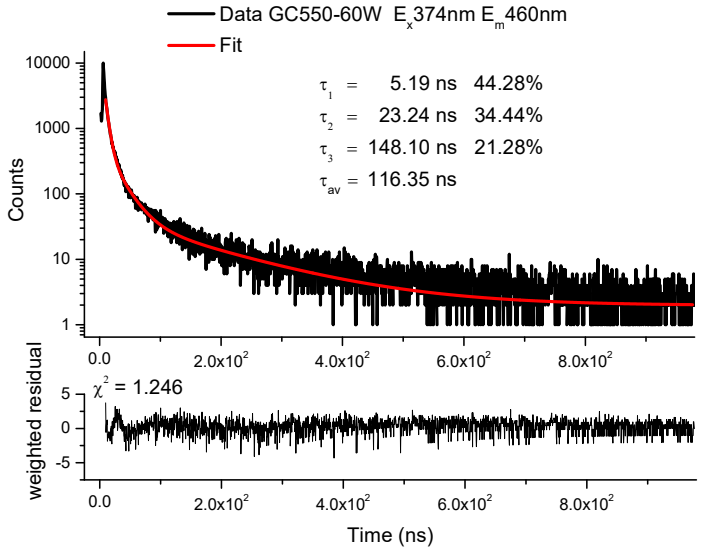

Figure S15. Lifetime measurement of GC550-60W. Emission 460 nm, Excitation 374 nm.

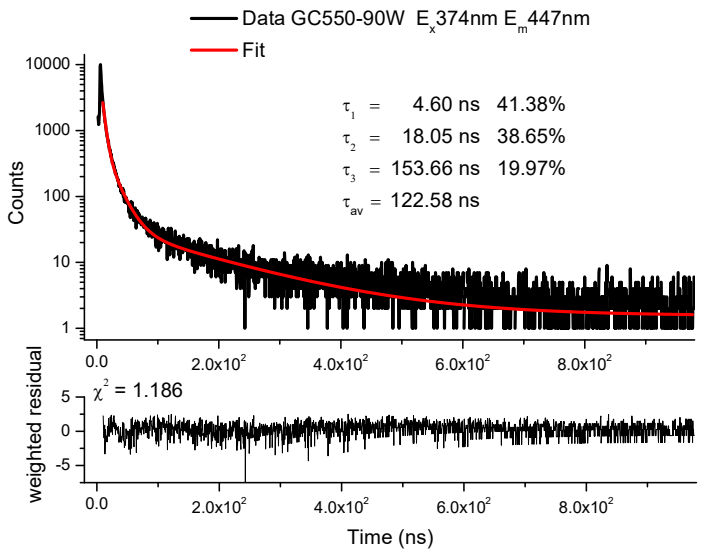

Figure S16. Lifetime measurement of GC550-90W. Emission 447 nm, Excitation 374 nm.

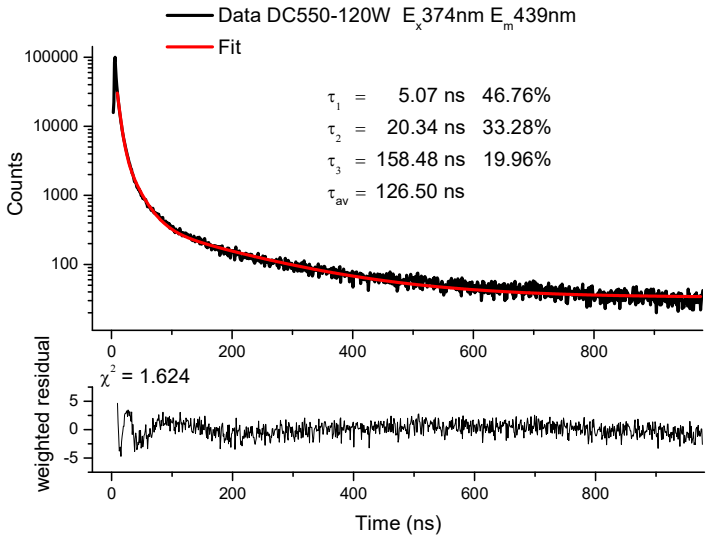

Figure S17. Lifetime measurement of GC550-120W. Emission 439 nm, Excitation 374 nm.

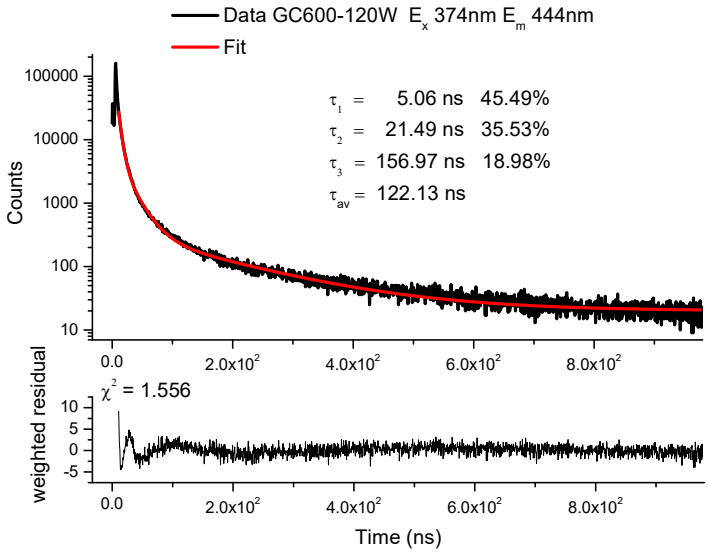

Figure S18. Lifetime measurement of GC600-120W. Emission 444 nm, Excitation 374 nm.

Table S1. Lifetime of the as-synthesized graphitic carbon nitride and US-exfoliated samples.

Sample	τ λ_{ex} =374 nm→ $\lambda_{em} = \lambda_{max}$		τ_{av} 374nm→λ_{max}
as-synthesized GC550	τ_1 = 8.11 ns τ_2 = 49.91 ns	55.69% 44.31%	42.82 ns
as-synthesized GC600	τ_1 = 7.94 ns τ_2 = 63.86 ns	53.12% 46.88%	56.96 ns
GC550-30W	τ_1 = 4.77 ns τ_2 = 19.73 ns τ_3 = 142.06 ns	50.09% 31.40% 18.51%	110.93 ns
GC550-60W	τ_1 = 5.19 ns τ_2 = 23.24 ns τ_3 = 148.10 ns	44.28% 34.44% 21.28%	116.35 ns
GC550-90W	τ_1 = 4.60 ns τ_2 = 18.05 ns τ_3 = 153.66 ns	41.38% 38.65% 19.97%	122.58 ns
GC550-120W	τ_1 = 5.07 ns τ_2 = 20.34 ns τ_3 = 158.48 ns	46.76% 33.28% 19.96%	126.50 ns
GC600-120W	τ_1 = 5.06 ns τ_2 = 21.49 ns τ_3 = 156.97 ns	45.49% 35.53% 18.98%	122.13 ns

N_2 physisorption analysis

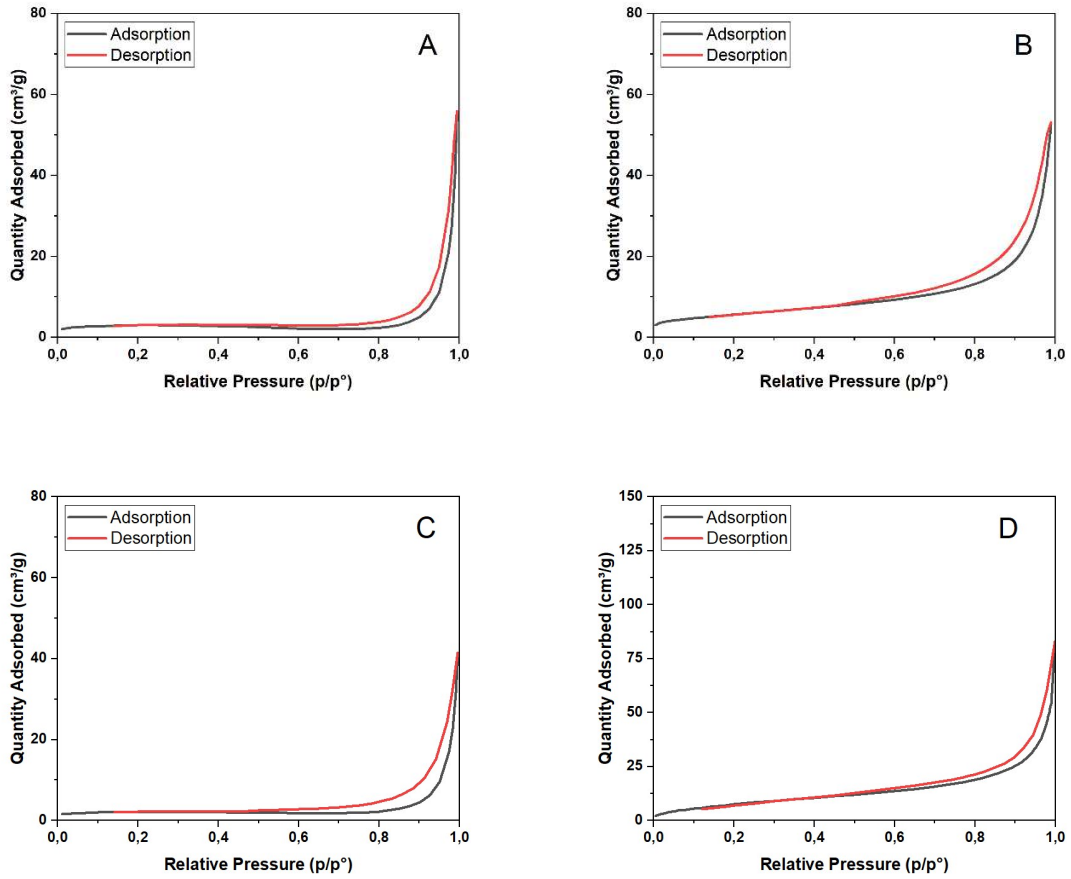

Figure S19. Adsorption and desorption isotherms for: A) GC-550; B) GC-550-120W; C) GC-600; D) GC-600-120W.

References

(1) Conte, F.; García-López, E. I.; Marcì, G.; Bianchi, C. L. M.; Ramis, G.; Rossetti, I. Carbon Nitride-Based Catalysts for High Pressure CO2 Photoreduction. *Catalysts* **2022**, *12* (12), 1628. https://doi.org/10.3390/catal12121628.

(2) Gesesse, G. D.; Gomis-Berenguer, A.; Barthe, M.-F.; Ania, C. O. On the Analysis of Diffuse Reflectance Measurements to Estimate the Optical Properties of Amorphous Porous Carbons and Semiconductor/Carbon Catalysts. *J. Photochem. Photobiol. A Chem.* **2020**, *398*, 112622. https://doi.org/10.1016/j.jphotochem.2020.112622.

(3) *Principles of Fluorescence Spectroscopy*; Lakowicz, J. R., Ed.; Springer US: Boston, MA, 2006. https://doi.org/10.1007/978-0-387-46312-4.

(4) Suzuki, K.; Kobayashi, A.; Kaneko, S.; Takehira, K.; Yoshihara, T.; Ishida, H.; Shiina, Y.; Oishi, S.; Tobita, S. Reevaluation of Absolute Luminescence Quantum Yields of Standard Solutions Using a Spectrometer with an Integrating Sphere and a Back-Thinned CCD Detector. *Phys. Chem. Chem. Phys.* **2009**, *11* (42), 9850. https://doi.org/10.1039/b912178a.

(5) Zhu, B.; Zhang, L.; Cheng, B.; Yu, J. First-Principle Calculation Study of Tri-s-Triazine-Based g-C3N4: A Review. *Appl. Catal. B Environ.* **2018**, *224*, 983–999. https://doi.org/10.1016/j.apcatb.2017.11.025.

(6) Bahadori, E.; Tripodi, A.; Villa, A.; Pirola, C.; Prati, L.; Ramis, G.; Rossetti, I. High Pressure Photoreduction of CO2: Effect of Catalyst Formulation, Hole Scavenger Addition and Operating Conditions. *Catalysts* **2018**, *8* (10), 430. https://doi.org/10.3390/catal8100430.